References

ABRAMOWITZ, M., & STEGUN, I. A. (1965). *Handbook of Mathematical Functions*, p. 297. New York: Dover.

AYRES, F. (1962). *Matrices*, p. 58. Schaum Publ. Co.

BLOW, D. M. & CRICK, F. H. C. (1959). *Acta Cryst.* **12**, 794.

CASTELLANO, E., PODJARNY, A. & NAVAZA, J. (1973). *Acta Cryst.* A**29**, 609–615.

COULTER, C. L. & DEWAR, R. B. K. (1971). *Acta Cryst.* B**27**, 1730–1740.

DESTRÓ, R. (1972). *Report CECAM Workshop*, p. 9.

GOEDKOOP, J. A. (1950). *Acta Cryst.* **3**, 374–378.

HENDRICKSON, W. A. & KARLE, J. (1973). *J. Biol. Chem.* **243**, 3327–3340.

KARLE, J. & HAUPTMAN, H. (1950). *Acta Cryst.* **3**, 181–187.

KARLE, J. & KARLE, I. L. (1966). *Acta Cryst.* **21**, 849–859.

KARTHA, G. (1967). *Nature, Lond.* **214**, 234–330.

MCLACHLAN, N. W. (1955). *Bessel Functions*, p. 202. Oxford: Clarendon Press.

MAIN, P. (1973). *Commun. CECAM Symposium*, Holland. p. 14.

MOULT, J., YONATH, A., TRAUB, W., SMILANSKY, A., PODJARNY, A. D., SAYA, A. & RABINOVICH, D. (1976). *J. Mol. Biol.* In the press.

NORTH, A. C. T. & PHILLIPS, D. C. (1969). *Prog. Biophys.* **19**, part 1, 1.

RANGO, C. DE, MAUGUEN, Y. & TSOUCARIS, G. (1975). *Acta Cryst.* A**31**, 227–233.

RANGO, C. DE, TSOUCARIS, G., & ZELWER, C. (1974). *Acta Cryst.* A**30**, 342–353.

REEKE, G. N. & LIPSCOMB, W. N. (1969). *Acta Cryst.* B**25**, 2614–2623.

SAYRE, D. (1953). *Acta Cryst.* **5**, 60–65.

SAYRE, D. (1974). *Acta Cryst.* A**30**, 180–184.

TSOUCARIS, G. (1970*a*). *Acta Cryst.* A**26**, 492–499.

TSOUCARIS, G. (1970*b*). *Acta Cryst.* A**26**, 499–501.

WEINZIERL, J. E., EISENBERG, D. & DICKERSON, R. E. (1969). *Acta Cryst.* B**25**, 380–387.

YONATH, A., SMILANSKY, A., MOULT, J. & TRAUB, W. (1973). *Abs. 9th. Int. Cong. Biochem.* Stockholm, p. 120.

Acta Cryst. (1976). A**32**, 292

Multiple Diffraction in Diamond*

BY BEN POST

Polytechnic Institute of New York, Brooklyn, N.Y. 11201, *U.S.A.*

(*Received* 2 *May* 1975; *accepted* 23 *September* 1975)

The 002 and 222 multiple diffraction patterns of diamond, originally recorded by Renninger [*Z. Phys.* (1937). **106**, 141–176.], have been reexamined using high-resolution techniques. Several previously unreported features of these patterns have been observed and are discussed.

Introduction

The first systematic investigation of multiple X-ray diffraction effects in single crystals was carried out by Renninger (1937). He recorded and analyzed the 002 and 222 multiple diffraction patterns of diamond crystals – using Cu $K\alpha$ and Mo $K\alpha$ radiations – in what is now generally regarded as a classic study of the phenomenon.

We have recently calculated the azimuthal angles at which multiple diffraction effects may be observed in 002 and 222 'Renninger patterns' of diamond, recorded with Cu $K\alpha$ radiation. These indicate that several features of crystallographic interest, in addition to those described by Renninger, would be revealed if the patterns were recorded with high-resolution techniques. Results of such an investigation are discussed below.

The geometry and intensities of multiple X-ray diffraction effects in single crystals have been discussed by many investigators in recent years, including: Cole, Chambers & Dunn (1962); Moon & Shull (1964); Zachariasen (1965); Caticha-Ellis (1969) and Prager (1971). An extensive bibliography of the subject is included in a review paper by Terminasov & Tuzov (1964), and more recent references are listed by Post (1975).

Experimental

The experimental arrangement used in this investigation is similar to Renninger's, modified to improve resolution (Fig. 1). The X-ray source was a Cu target tube with an effective focal spot size of 400×500 μm at a take-off angle of 4°. A 0·5 mm pinhole at the exit end of a 120 cm evacuated tube between the source and the specimen limited the divergence of the incident beam to 2′ of arc.

Two diamond specimens were used. One was a 1 cm square platelet, 2 mm thick, with [001] normal to the large face. It was optically clear and colorless, and exhibited considerable birefringence when examined between crossed polarizers. The other was roughly octahedral in shape, with triangular (111) faces ap-

* Work supported in part by: Contract F44620-74-C-0065, U.S. Army, Joint Services to the Electronics Program.

proximately 4 mm on edge. It was faintly amber in transmitted light and displayed very weak birefringence.

Precise alignment of the specimen is essential for multiple diffraction studies. It is first tilted about the normal to the plane of incidence to bring the 'primary' reflecting planes to their diffracting position (Fig. 1). The arcs of the crystal holder are then adjusted until the diffraction vector of the reflecting planes is precisely parallel to the crystal rotation axis. That setting is considered satisfactory when the diffracted intensity does not vary by more than about 10% as the crystal is rotated through 360°, except for possible abrupt changes due to multiple diffraction. The inclination of the rotation axis is then readjusted to maximize the multiple diffraction intensities.

A scintillation detector is used to monitor the intensity of the primary reflection while the crystal is rotated slowly about its axis. As the crystal rotates, reciprocal lattice points pass through their diffracting positions on the surface of the Ewald sphere, generating 'secondary' reflections. The effects of the latter on the primary diffracted intensity (*i.e.* on the 'background' intensity) constitute the multiple diffraction effects to be investigated.

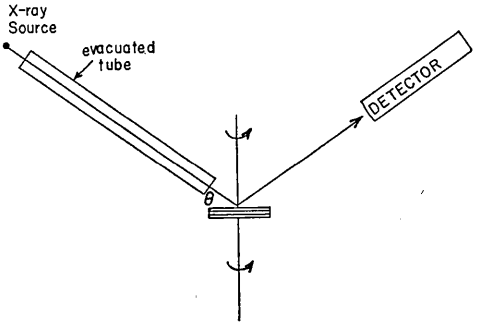

Fig. 1. Experimental setup (schematic).

Results and discussion

(*a*) *The* (002) *patterns*

Asymmetric, 45° portions of the 002 multiple diffraction patterns of diamond, recorded with Cu $K\alpha_1$ and $K\alpha_2$ radiations, are shown in Figs. 2 and 3. The calculated values of the azimuthal angles of the multiple diffraction maxima are listed in Table 1. The indices of the secondary reflections involved in each interaction are listed on the figures. To minimize confusion, the indices of the incident beam and the primary reflection, (000) and (002), have been omitted although they are involved in all the interactions.

Table 1. *Calculated azimuthal angles of* 002 *multiple diffraction peaks*

hkl	*n*	Azimuthal angle Cu $K\alpha_1$	Cu $K\alpha_2$
222/220	4	2·370	2·208
$3\bar{1}\bar{1}/3\bar{1}3$	4	8·292	9·322
$1\bar{1}\bar{1}/1\bar{1}3$	4	12·842	13·122
400/402	4	16·705	16·111
$1\bar{3}1$	3	24·525	24·688
$3\bar{1}\bar{1}/3\bar{1}3$	4	28·579	27·548
311	3	28·605	28·442
$0\bar{2}0/0\bar{2}2$	4	27·614	28·709
$3\bar{3}\bar{1}$	3	28·630	29·237
111	3	35·252	35·222

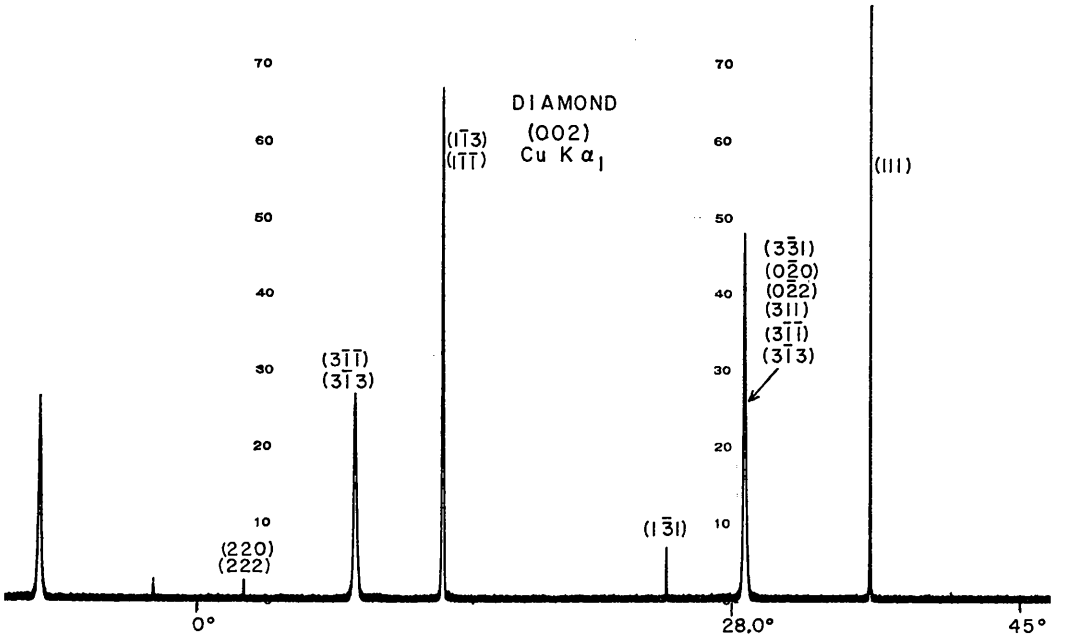

Fig. 2. 002 multiple diffraction pattern of diamond: Cu $K\alpha_1$.

The arrow at the base of the $3\bar{1}1/313$ peak on Fig 3 points to a bump in the background intensity, caused by the corresponding $K\alpha_1$ peak, which we could not entirely eliminate.

An unusual peak appears on Fig. 2 at the azimuthal angle of 28·6°. Six sets of *hkl* indices are listed for that maximum. The latter is due to overlap of four independent maxima which occur within the angular range 28·58° to 28·63° in the $K\alpha_1$ pattern (Table 1). Those include two four-beam and two three-beam interactions. In the $K\alpha_2$ pattern, the 'single' $K\alpha_1$ peak is resolved into its four component peaks and it is clear that their apparent coincidence in Fig. 2 is accidental.

It will be noted that more four-beam than three-beam interactions are listed on Figs. 2 and 3. This is a consequence of the fact that in those cases the rotation axis, *c*, is parallel to *c**, and passes through the origins of successive reciprocal lattice levels (Fig. 4). When the crystal is set to record 002 patterns, reciprocal lattice points with *l* equal to 1 lie in the equatorial plane of the Ewald sphere and participate in three-beam interactions: (000,002,*hkl*). The *l* indices of most reciprocal lattice points, however, do not equal 1; these arrive at their diffracting positions accompanied by their geometrical counterparts with $l=2-l'$, and four-beam or higher-order diffraction results.

The weak 000, 002, 220, 222, four-beam interaction (Fig. 2, at 2·37°) has not been reported previously. It is an example of the geometry discussed in the preceding paragraph and illustrates what Zachariasen (1965) has referred to as 'the case of triple-diffraction, with $\mathbf{H}_1 \cdot \mathbf{H}_2=0$ and $\mathbf{H}_3=\mathbf{H}_1+\mathbf{H}_2$'. [$\mathbf{H}_1$, $\mathbf{H}_2$ and $\mathbf{H}_3$ correspond to the diffraction vectors of our 002, 220 and 222.*] The contribution of this four-beam interaction to the 002 primary reflection would equal zero if the structure factors of both 002 and 222 equalled zero [Moon & Shull (1964), equation 9]. The structure factor of 002 does indeed equal zero, but that of 222, though very weak, differs sufficiently from zero to generate the weak maximum that is observed.

The argument outlined above appears to be inconsistent with the observation of the 000, 002, $0\bar{2}0$, $0\bar{2}2$ maximum at 28·71° (Fig. 3); the structure factors

* The 000 term was not included explicitly in Zachariasen's 'triple-diffraction'.

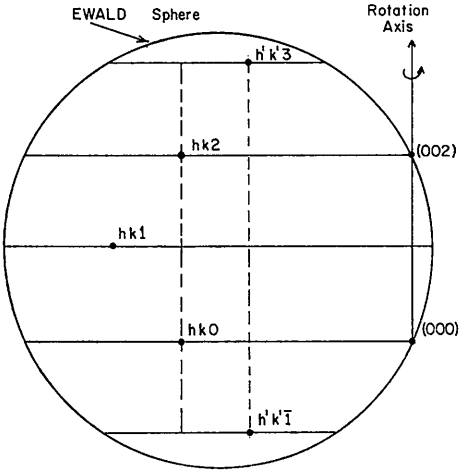

Fig. 4. Multiplicity of reflections.

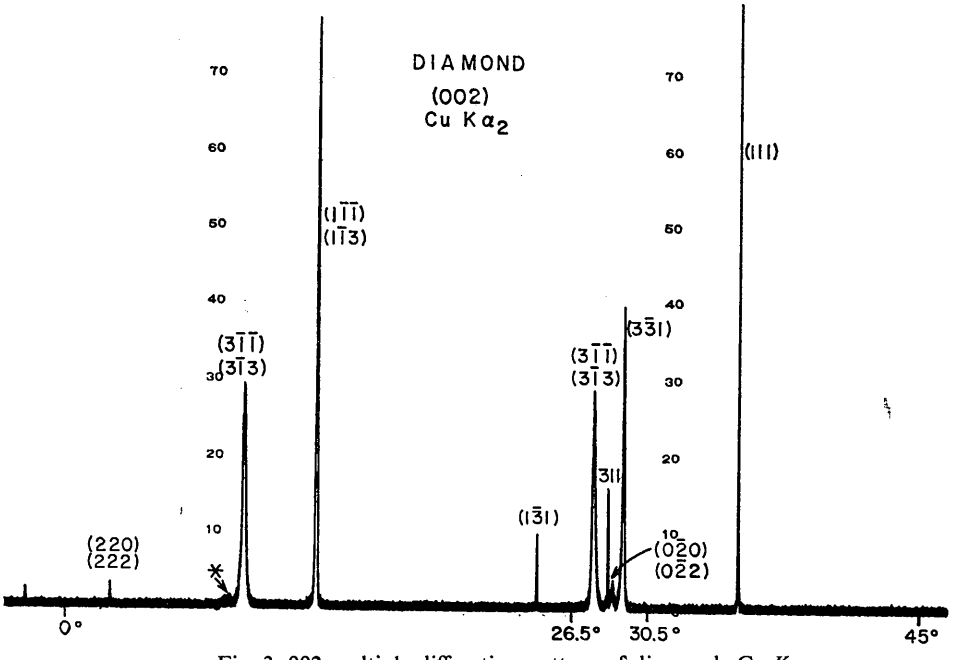

Fig. 3. 002 multiple diffraction pattern of diamond: Cu $K\alpha_2$.

of *both* 002 and $0\bar{2}0$ equal zero in cubic diamond crystals. It will be recalled, however, that the specimen used for the 002 patterns was optically birefringent. Kleinman (1962) has discussed deviations from cubic symmetry resulting from residual strain effects in diamond crystals. In such cases, the crystal is not only birefringent, but the intensities of reflections, such as $0\bar{2}0$, which are 'forbidden' in *cubic* crystals, may no longer equal zero. That could account for the weak maximum at 28·71°. This intensity effect appears, in this case at least, to be limited to the *hk*0 zone of reflections. For example, no evidence of a diffraction maximum due to 002 could be detected.

(b) The (222) *pattern*

Fig. 5 is a chart recording of the 222 multiple diffraction pattern obtained using Cu $K\alpha_1$; the asymmetric 30° portion of the recording is shown. The outstanding features are the intense 313, 113, $\bar{3}13$ peaks; these were observed and discussed by Renninger (1937). The extraordinary width of the 313 peak is due to an unusually large Lorentz factor (25·6); the corresponding reciprocal lattice point enters and leaves the Ewald sphere within a total angular range of less than 10°. It does not touch the $K\alpha_2$ sphere at any point and 313 is, of course, absent from the $K\alpha_2$ pattern.

The minima due to the 000, 222, 220, 402 and the 000, 222 002, 220 interactions (Fig. 5) have been reported by Renninger (1955). He attributed them to 'aufhellung' effects resulting from simultaneous diffraction by the primary 222 reflection and the very strong 220. That interpretation, unfortunately, overlooks the four-beam character of the interactions, as well as the interesting relation between the umweg *minimum* due to 000, 222, 220, 002 on Fig. 5 and the *maximum* due to the same group of reflections on Fig. 1 (See Fig. 6).

(c) Intensities of the weak interactions

Moon & Shull (1964) and Zachariasen (1965) have described procedures for the calculation of multiple diffraction intensities in *mosaic* crystals. These methods may also be used for the calculation of weak interactions in relatively perfect crystals, such as diamond. Hirsch & Ramachandran (1950) have shown that intensity calculations based on either perfect or mosaic crystal formulae lead to essentially identical results for very weak reflections. We have therefore restricted our calculations to the five weakest interactions observed in Figs. 3 and 5. We feel that the quality of the intensity data for the stronger interactions did not warrant more detailed dynamical intensity calculations for those cases.

Intensities were measured by scanning repeatedly across the maxima (or minima) until accumulated net 'counts' equalled 3000. Since the divergence of the incident beam equalled 2′ of arc and exceeded the acceptance angles of the weak interactions by large margins, *integrated* intensities were measured in the scanning process. The resultant precision was not high; our estimates of the standard errors of these measurements range from about 25% for the 002 cases to 40% for the 222 interactions.

The measured values were placed on a common scale by equating the *peak* intensities of the 000, 002, 220, 222 interaction of Fig. 3 with that of the 000, 222, 220, 002 of Fig. 5. Equation 9 of Moon & Shull's (1964) paper shows that the two interactions should yield

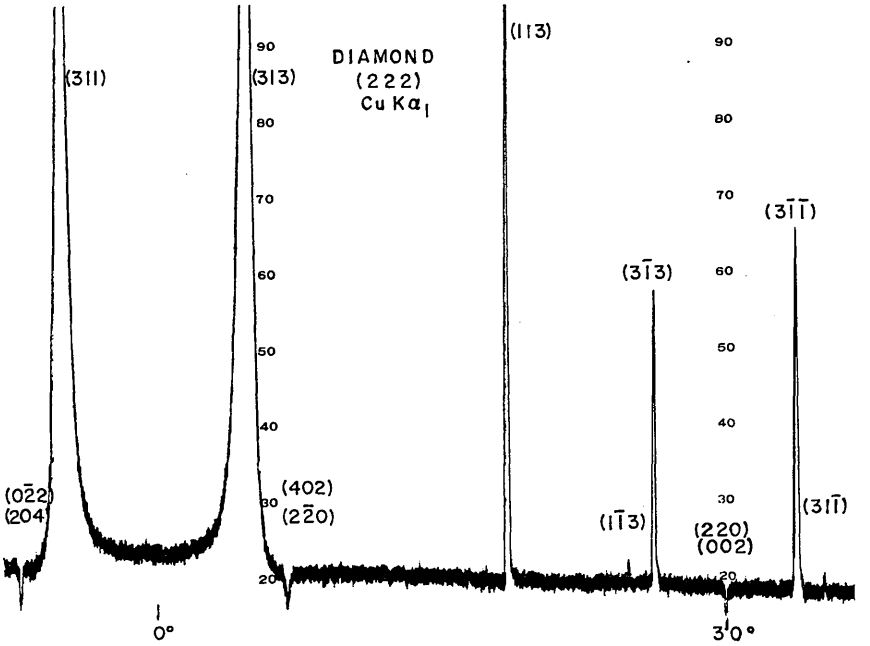

Fig. 5. 222 multiple diffraction pattern: Cu $K\alpha_1$.

identical peak intensities; their *integrated* intensities will differ as a result of differences between their Lorentz factors. The integrated intensities of the Fig. 3 maximum were then arbitrarily set to equal 10·0.

Table 2. *Integrated intensities of weak multiple diffraction interactions*

Primary reflection	Secondary reflections	Radiation	Relative intensities Measured	Calculated
222	402, $2\bar{2}0$	Cu $K\alpha_1$	−35	−46·5
	220, 002	Cu $K\alpha_1$	−15	−20·6
	$1\bar{1}3$	Cu $K\alpha_1$	8	6·9
002	220, 222	Cu $K\alpha_2$	10	10·0
	$0\bar{2}0$, $0\bar{2}2$	Cu $K\alpha_2$	30	0*

* Calculated value equals zero for *unstrained* cubic crystals. See text for discussion.

Calculated and measured integrated intensities of the five weak interactions are listed in Table 2. The negative intensity values indicate decrease of the primary 222 intensity. The calculations were based on Moon & Shull's (1964) procedure, modified to include polarization corrections as described by Zachariasen (1965):

$$I_{(\text{integ})} = \frac{Q_1}{2}\sum_i \left\{ -\frac{Q_i}{K_i}\left[p_{1,i}(i-1)\right] - \frac{Q_{(i-1)}}{K_{(i-1)}}\left[p_{1,i-1}\{(i-1)-1\}\right] + \left[K_i^2+K_{1-i}^2\right]^{-1/2}\left[\frac{Q_iQ_{1-i}}{Q_1}\right]\left[p_{i,i-1}\{(i-1)-i\}\right]\right\}. \quad (1)$$

Subscript 1 refers to the indices of the primary reflection; i refers to the indices of the secondary reflection(s), $Q_i=(\lambda^3N^2|F|^2/\sin 2\theta)_i$, $p_{i,j}(j-i)=\frac{1}{2}[\cos^2 2\theta_i+\cos^2 2\theta_j+(\cos 2\theta_{j-i}-\cos 2\theta_i\cos 2\theta_j)^2]$, and $K_i=1/(\sin 2\theta_i)$ (Lorentz factor)$_i$.

The weak $1\bar{1}3$ maximum in Fig. 5 is of some interest. It results from interchanges of intensity among the incident beam and 222, $1\bar{1}3$ and $13\bar{1}$ [the latter represents the index of P as viewed from H, Fig. 7; it is referred to as $(1-i)$ in equation 1]. The values of 2θ of the three reflections, for Cu $K\alpha_1$, are 96·84, 91·48, and 91·48°. The polarization correction reduces the contribution of $1\bar{1}3$ to 222 (*via* $13\bar{1}$) to 0·007 times its uncorrected value, resulting in the $1\bar{1}3$ maximum which is observed to be vanishingly weak.

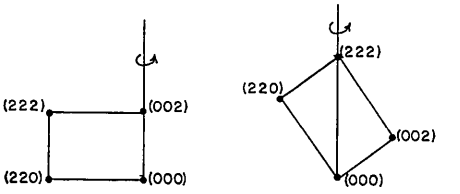

(*a*) (*b*)

Fig. 6. Identical four-beam interactions in different orientations.

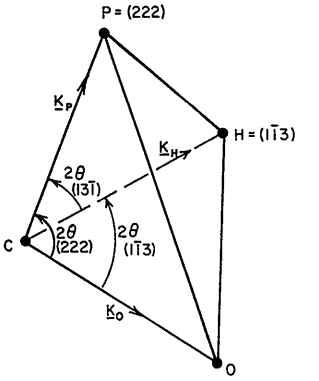

Fig. 7. Geometry of 222/$1\bar{1}3$ interaction.

References

CATICHA-ELLIS, S. (1969). *Acta Cryst.* A**25**, 666–673.

COLE, H., CHAMBERS, F. W. & DUNN, H. M. (1962). *Acta Cryst.* **15**, 138–144.

HIRSCH, P. B. & RAMACHANDRAN, G. N. (1950). *Acta Cryst.* **3**, 187–194.

KLEINMAN, L. (1962). *Phys. Rev.* **128**, 2614–2619.

MOON, R. M. & SHULL, C. G. (1964). *Acta Cryst.* **17**, 805–812.

POST, B. (1975). *J. Appl. Cryst.* **8**, 452–456.

PRAGER, P. R. (1971). *Acta Cryst.* A**27**, 563–569.

RENNINGER, M. (1937). *Z. Phys.* **106**, 141–176.

RENNINGER, M. (1955). *Acta Cryst.* **8**, 606–610.

TERMINASOV, Y. S. & TUZOV, L. V. (1964). *Usp. Phys. Nauk.* **83**, 223–258.

ZACHARIASEN, W. H. (1965). *Acta Cryst.* **18**, 705–710.